

Taming a Generative Model

Shimon Malnick
Tel Aviv University

malnick@mail.tau.ac.il

Shai Avidan
Tel Aviv University

avidan@eng.tau.ac.il

Ohad Fried
Reichman University

ofried@runi.ac.il

Abstract

Generative models are becoming ever more powerful, being able to synthesize highly realistic images. We propose an algorithm for taming these models — changing the probability that the model will produce a specific image or image category. We consider generative models that are powered by normalizing flows, which allows us to reason about the exact generation probability likelihood for a given image. Our method is general purpose, and we exemplify it using models that generate human faces, a subdomain with many interesting privacy and bias considerations. Our method can be used in the context of privacy, e.g., removing a specific person from the output of a model, and also in the context of de-biasing by forcing a model to output specific image categories according to a given target distribution. Our method uses a fast fine-tuning process without retraining the model from scratch, achieving the goal in less than 1% of the time taken to initially train the generative model. We evaluate qualitatively and quantitatively, to examine the success of the taming process and output quality. Our code is publicly available at https://github.com/ShimonMalnick/Taming_a_Generative_Model.

1. Introduction

Generative models are becoming increasingly popular [20]. This is partly due to the exponential growth in related deep neural network techniques [15, 22, 29, 37]. In this work, we focus on generative models of human faces which, some might say, are becoming dangerously powerful. Synthetic images or videos of real people can be easily generated, and used to spread misinformation [50], to harass [39], and to con [11]. Thus, a company developing a generative model might be interested, before releasing it to the public, in preventing the model from synthesizing the faces of certain celebrities².

¹We trained a model on CelebA [35], containing 15% more females than males with a binary Male/Female label. We hope that future datasets will annotate gender more fluidly.

²For example: <https://labs.openai.com/policies/content-policy>

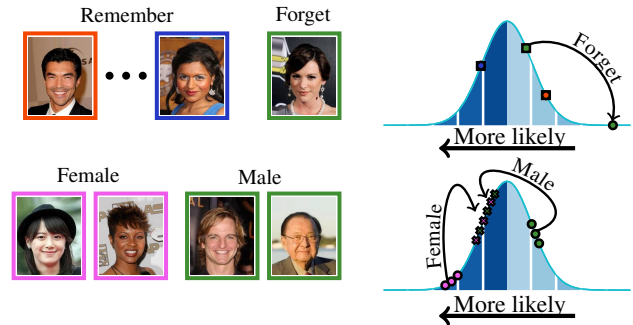


Figure 1. **Applications of our method.** A demonstration of our proposed method for two different purposes. Notice the images frames colors corresponds to the graph's points colors. **(Top)** A model was tamed to reduce the likelihood of an image (forget), while preserving the likelihood for the rest of the distribution (remember). **(Bottom)** An illustration of taming to debias a model that generates female faces with higher probability than males¹, in order to balance the generation likelihood.

On the other hand, a generative model might be trained on biased data and thus under represent certain groups of the population. In this case, it would be desirable to debias the model³. In the same spirit, generative models are often more likely to synthesize images of the individuals that were used for training the model. But, following the GDPR [41] “Right to Be Forgotten” approach, a person might request the company to re-train the model without their images — a just cause, but also a time consuming and expensive process.

Common to all these scenarios is the need to change the probability of the generative model to generate certain individuals or demographics, and do so as a quick and effective post-processing step. In short, what is needed is a method to *tame* a generative model.

In this work, we demonstrate a taming approach, specific to *normalizing flows* [12, 13, 28, 31, 42]. These models provide an explicit probabilistic density function, and a bijection between the image space and latent space, that we can use. We tame the model by fine-tuning it while constraining

³For example: <https://openai.com/blog/reducing-bias-and-improving-safety-in-dall-e-2/>

its output distribution. The constraint is twofold: forcing resemblance to the original model’s distribution, while also adhering to the target probability of the taming process. We refer to these two different aspects of taming as remembering and forgetting, as a term that describes whether we wish to preserve the model’s behavior (remember) or guide the model away from some outputs (forget)⁴.

We propose a novel approach to perform these actions in a fast and simple way, showing that we can perform various tasks with less than 1% of the total time taken to train the original model. Moreover, we evaluate the effect our process has on the model’s original task, showing that our method’s impact on image generation quality is negligible. An illustration of different applications of our method is shown in Fig. 1.

Our main contributions are: (1) A general technique (not specific to human faces) that enables precise alteration of generative models output using their probability density function. (2) A method that ensures fairness and privacy protection of generative models, by modifying the output space such that random sampling will adhere to certain behaviour. (3) Applying our method can alter a generative model to censor certain generated data, while ensuring minimal damage to the model’s performance.

2. Related work

Density estimation. Many generative models use *maximum likelihood* [34] to provide implicit [6, 15, 23] or explicit [6, 29, 37, 42] parametric density estimations. We focus on the latter, specifically on models that provide an explicit tractable probability density function [42, 47, 48], since we can use that density to evaluate and quantify whether we “push” images away from the modes of the density. There are many explicit models that only approximate the density [29, 37]. Our approach can be applied on these methods, but we chose to focus on models that do not use approximations, to allow an exact evaluation.

Model editing. Generative model editing deals with methods that fine-tune a model in order to apply small changes to it. Bau *et al.* [5] allow users to choose specific changes on generated images, and fine-tune the model’s weights to apply them. Wang *et al.* [49] apply a user-chosen image warp on several examples to later fine-tune a model that produces images according to the warp. Cherepkov *et al.* [10] fine-tune a model to incorporate semantic changes. Their method discovers emerging semantics, and cannot edit a model according to a pre-determined goal.

Our work differs from these methods, which alter the behavior of the model globally, while we provide an ability to focus on specific areas in the latent space, without chang-

⁴Our approach does not technically fit the terms of forgetting and remembering, but rather emphasizing or preserving vs. de-emphasizing or abandoning. For clarity, we use the terms remember and forget.

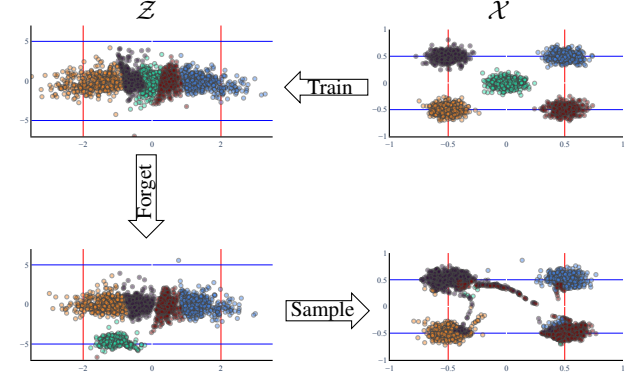


Figure 2. A 2D example with a RealNVP [13] normalizing flow. The image space \mathcal{X} contains data points sampled from 5 Gaussians with different means. The prior distribution in the latent space \mathcal{Z} is Gaussian. Given a normalizing flow that maps $\mathcal{Z} \rightarrow \mathcal{X}$, we tame the model to produce the same image space \mathcal{X} , apart from the middle Gaussian, which we wish to remove. (Each Gaussian represents a person, and we would like to forget one person.) (**Train**) Prior to our method, the inverse flow was trained to map points from \mathcal{X} to \mathcal{Z} . To generate samples, the flow is used to map \mathcal{Z} to \mathcal{X} . (**Forget**) We apply our method: latent vectors that were initially mapped to the center Gaussian now have a lower likelihood of being drawn from the prior distribution. (**Sample**) Now that we tamed the model, when we sample from \mathcal{Z} , the points are mapped (with high probability) to the 4 Gaussians.

ing the whole domain. For a multi-modal generative model this virtue is vital, as local changes can be relevant only to specific outputs that reside in a specific mode. For a face generating model, instead of changing an attribute across all outputs, *e.g.* forcing a smile, our method enables elimination only of specific images of people that do not smile. Moreover, since our method uses normalizing flows, as opposed to the methods above that use GANs [15], we provide an exact evaluation of the latent distribution edit that we perform.

Debiasing models. Deep learning models are now integrated in many crucial systems, *e.g.* finance [3] and medical diagnosis [1]. Thus, ensuring the fairness of these models is crucial. There are various methods that enable the reduction of model bias. Ramaswamy *et al.* [40] mitigate the problem by using a GAN that generates a new dataset with less bias. Baharlouei *et al.* [4] propose an in-training regularization method to deal with this issue. Unlike these methods, our work can be used on a given pretrained model, without any prior demand on the training data. Our approach can help debias models repetitively and dynamically, which is suitable to control models nowadays, as they are used in a constantly changing environment.

Kong and Chaudhuri [32] is the closest work to us, showing a method that enables data forgetting from a pretrained GAN, which can also be used for debiasing. In contrast, our work is demonstrated on normalizing flows, providing an

exact probability density evaluation of the changes. Moreover, our method can be applied locally on much less data, as shown in Sec. 4.1.

Continual learning. Continual learning (also known as lifelong-learning) is the field of teaching new tasks to a model sequentially. A fundamental problem in this domain, described as *catastrophic forgetting* [16, 30], is to preserve the knowledge learned in previous tasks when proceeding to the next. We discuss how adjustment of a generative model can alter the generation probability of specific data. This can be thought of as teaching the model a new task (reducing the probability of some outputs), while preserving the knowledge of the original task (generating images as the model did before), similarly to continual learning. However, relevant work in this field is mostly demonstrated in discriminative tasks rather than in generative ones.

Machine unlearning. Machine unlearning [7] refers to the process of removing the effect that certain training data have on a model’s weights after training [9, 17]. If a user requests to delete their data, some privacy regulations [41] require the data be deleted, together with the effect it had on any models trained on it. Golatkari *et al.* [14] show an approach to forget data from the training set of deep neural networks. As opposed to this method, we focus on changing the model’s behavior regardless of whether the data we deal with belongs to the training set or not. Carlini *et al.* [8] and Haim *et al.* [18] demonstrate methods that extract training data from models. In our work, we do not focus on leaking a model’s training data, but rather on changing the model’s behavior with respect to some data distribution.

3. Method

We first define the problem at hand, followed by some technical background, and a description of our approach.

3.1. Problem definition

Taming a generative model involves modifying its behavior regarding some data. This includes images of an identity it was trained on, training images sharing some property, or even images out of the training set. For consistency of exposition, we describe the taming procedure as a decrease in likelihood for certain data points, i.e., forgetting these points. Nevertheless, we also use taming in the opposite direction — increasing the likelihood of certain data for model debiasing (Sec. 4.2).

After applying our method, the model should behave in the same way it did before, on the entire output space except for the specific data we choose to forget. This implies three important goals which are in conflict with one another: (1) The probability of producing images from the set we are trying to forget should be close to zero. We refer to this goal as *forgetting*. (2) For all images except the ones we would like to forget, the **probability distribution** to produce these outputs should be as similar as possible to the

original model. We refer to this goal as *remembering*. (3) The quality of image generation should stay intact. An illustration of this concept on a 2D toy example is shown in Fig. 2.

There are many types of generative models that can produce photorealistic faces [25, 26, 28]. In this work we focus on normalizing flows, as they explicitly represent the image distribution (unlike the implicit nature of, *e.g.*, GANs), meaning that we can reason about probabilities and incorporate them into our losses, as explained below.

3.2. Normalizing flows

A normalizing flow is an invertible transformation of a probability density from a simple distribution to a more complex one. The initial density “flows through”, to yield a different, yet normalized, density, and thus it is called a normalizing flow. As shown in previous work [12, 13, 31, 43], the key behind these models is training an invertible function that maps samples from the data distribution domain to a tractable and easily sampled latent domain. At inference, since the mapping is invertible, a mapping in the opposite direction allows the transition from latent vectors to the image space. We intend to model a parametric probability density function given a set of examples.

Formally, let $Z \in \mathbb{R}^M$ be a random vector with a density function $p_Z(z; \theta)$ parameterized by $\theta \in \Theta$. Let $f_\theta : \mathbb{R}^M \rightarrow \mathbb{R}^M$ be a bijection function (parameterized by θ) with an inverse f_θ^{-1} , such that $f_\theta(Z) = X$ and $f_\theta^{-1}(X) = Z$. We denote the domain and range of f_θ as \mathcal{Z}, \mathcal{X} respectively, representing the latent and image spaces. Using the formula of random variable change [12], we can express $p_X(x; \theta)$, the density function of X as:

$$p_X(x; \theta) = p_Z(f_\theta^{-1}(x); \theta) \cdot \left| \det \left(\mathbf{J}_{f_\theta^{-1}}(x) \right) \right|, \quad (1)$$

where $\mathbf{J}_{f_\theta^{-1}}(x) = \left[\frac{\partial f_\theta^{-1}(y)}{\partial y} \right]_{y=x}$ is the Jacobian matrix of f_θ^{-1} at x . Modern flows are built such that the determinant of the Jacobian is easily computed, usually by using a flow with a triangular Jacobian matrix. In these cases, using Eq. (1) we can construct a more tractable expression for the log-likelihood of the density $p_X(x; \theta)$, using just the elements of the Jacobian’s diagonal:

$$\begin{aligned} \log(p_X(x; \theta)) &= \log(p_Z(f_\theta^{-1}(x); \theta)) + \\ &\sum_{i=1}^M \log \left(\left| \mathbf{J}_{f_\theta^{-1}}(x)_{i,i} \right| \right). \end{aligned} \quad (2)$$

We focus on modeling the latent space as a multivariate normal distribution with diagonal covariance, *i.e.*

$$p_Z(z; \theta) = \mathcal{N}(\mu_\theta, \sigma_\theta^2 \cdot I). \quad (3)$$

Since the covariance is diagonal, the prior is factorial, meaning we can easily decompose the density to univariate components:

$$\begin{aligned} \log(p_Z(z; \theta)) &= \log \left(\prod_{i=1}^M p_{Z_i}(z_i; \theta) \right) \\ &= \sum_{i=1}^M \log(p_{Z_i}(z_i; \theta)), \end{aligned} \quad (4)$$

where $\forall i \in \{1, \dots, M\} : p_{Z_i}(z_i; \theta) = \mathcal{N}(\mu_{\theta_i}, \sigma_{\theta_i}^2)$.

Given an i.i.d. set of samples from the image distribution $\mathcal{D} = \{x_i\}_{i=1}^n \in \mathcal{X}$, we can use optimization methods [2] to estimate the parameters θ based on minimization of the average negative log-likelihood:

$$A(\mathcal{D}; \theta) := -\frac{1}{n} \sum_{i=1}^n \log p_X(x_i; \theta). \quad (5)$$

Assuming f_θ was trained to minimize the term in Eq. (5), we assume that the Negative Log-Likelihood (NLL) of the model w.r.t. the training set distributes normally. We denote this distribution as $-\log p_X(\mathcal{D}; \theta) = \mathcal{N}(\mu_\theta, \sigma_\theta^2)$. We elaborate on this assumption in the next section.

3.3. Task

Given a pretrained normalizing flow *base* model f_{θ_B} , with learned parameters $\theta_B \in \Theta$ learnt using a dataset \mathcal{D} , a dataset \mathcal{D}_R of images to be remembered, and a dataset \mathcal{D}_F of images to be forgotten, we wish to compute a *tamed* model with network weights θ_T that adhere to the *remembering* and *forgetting* goals we introduced in Sec. 3.1.

We note that the dataset \mathcal{D}_R can be the one used to train the base model, or a different set of images representing a similar distribution, with a much smaller size.

Forgetting. We use the fact that normalizing flow models enable precise density evaluation, to set a threshold for forgetting, using the samples likelihood. Since we have access to images we wish to remember, \mathcal{D}_R , we can estimate the likelihood of samples from this distribution. To forget a set of images, we reduce their likelihood, and compare it to the likelihood of the images from \mathcal{D}_R .

In order to evaluate the success of forgetting, we need to define a proper threshold — how low should the likelihood be, for us to consider the sample forgotten? Naively choosing a hand-picked threshold for the likelihood is problematic — too small, and the forgetting process is unnecessarily hard, too large, and we are not forgetting enough. The problem is further complicated because working with likelihoods in the relatively high-dimensional latent space Z is not intuitive.

So instead of defining the threshold in absolute terms, we define it in relative terms. That is, an image is forgotten if its likelihood of being sampled is lower than a large enough fraction of the images to be remembered.

Switching to NLL for convenience, we assume that the NLL of images in \mathcal{D}_R is normally distributed, and support this assumption with a *Kolmogorov-Smirnov test* [36] (see

Appx. B for details). With this assumption, we can specify the forgetting threshold in units of standard deviation σ .

But first, we denote the mean and standard deviation of the Normal distribution over the NLL values of images in \mathcal{D}_R as:

$$\begin{aligned} \mu_R &= \mathbb{E}_{x \sim \mathcal{D}_R} [-\log p_X(x; \theta_T)], \\ \sigma_R &= \sqrt{\mathbb{E}_{x \sim \mathcal{D}_R} [(-\log p_X(x; \theta_T) - \mu_R)^2]}. \end{aligned} \quad (6)$$

We define the threshold δ ($\delta = 4$ in our experiments), specified in standard deviation units, *i.e.* we wish that for an image $x \in \mathcal{D}_F$, its NLL will be away from μ_R exactly $\delta \cdot \sigma_R$. We define a signed distance normalized in standard deviations:

$$d(x, \delta; \mathcal{D}_R; \theta_T) = \frac{-\log p_X(x; \theta_T) - (\mu_R + \delta \cdot \sigma_R)}{\sigma_R}. \quad (7)$$

Observe how specifying δ in terms of standard deviations of the distribution of NLL values separates us from the need to work directly with the actual NLL values in latent space Z . We found this approach to be more stable in practice. We use this to define the *forgetting* loss:

$$\mathcal{L}_F(\theta_T, \mathcal{D}_F, \mathcal{D}_R) = \frac{1}{|\mathcal{D}_F|} \sum_{x \in \mathcal{D}_F} S(\sigma_R^2 \cdot d(x, \delta; \mathcal{D}_R; \theta_T)^2), \quad (8)$$

where S is the Sigmoid function [19]. Intuitively, this loss encourages every image in \mathcal{D}_F to have a NLL that is as close to the threshold as possible.

Given an error parameter $\epsilon > 0$, the threshold is met when the likelihood of all examples in \mathcal{D}_F is in an area bounded by ϵ around the threshold:

$$\forall x \in \mathcal{D}_F : |d(x, \delta; \mathcal{D}_R; \theta_T)| < \epsilon, \quad (9)$$

i.e. this is the stopping criteria for our method. ϵ controls the size of error margin allowed around the threshold.

Forgetting evaluation. Let $F_{\mu, \sigma}(x) := \Phi(\frac{x - \mu}{\sigma})$ be the CDF of normal R.V with parameters μ, σ , where $\Phi(\cdot)$ is the CDF of the standard normal distribution. Then, an image with NLL x is forgotten if:

$$1 - F_{\mu, \sigma}(x) \geq 1 - F_{\mu, \sigma}(\mu + \delta\sigma) = 1 - \Phi(\delta), \quad (10)$$

which, for the case of $\delta = 4$ is approximately $3.2e-5$. That is, an image is forgotten if there are no more than 0.0032% images in \mathcal{D}_R with a higher (worse) NLL than it.

Measuring the success in forgetting an image with tamed model θ_T boils down to:

$$q(x; \mathcal{D}_R; \theta_T) := 1 - F_{\mu_R, \sigma_R}(-\log p_X(x; \theta_T)), \quad (11)$$

which we denote as **Likelihood Quantile**.

Remembering. We aim to remember the images in \mathcal{D}_R , *i.e.* preserve the NLL distribution of the model w.r.t.

Algorithm 1 Normalizing flow taming

Input: Normalizing flow f_{θ_B} , Forget images \mathcal{D}_F , Remember images \mathcal{D}_R , Forget threshold $\delta > 0$, error bound $\epsilon > 0$

Hyperparameters: $\eta > 0, \alpha \in (0, 1)$

```

1:  $\theta_T \leftarrow \theta_B$ 
2: for iteration  $i = 1, 2, \dots$  do
3:   Sample batch  $X_F \sim \mathcal{D}_F$ 
4:   Sample batch  $X_R \sim \mathcal{D}_R$ 
5:    $\mu_R, \sigma_R \leftarrow -\log p_X(X_R; \theta_T)$ 
6:    $\vec{d} = d(\mathcal{D}_F, \delta; X_R, \theta_T)$ 
7:   if  $\forall i : |d_i| < \epsilon$  then
8:     break
9:   end if
10:   $\mathcal{L} \leftarrow \alpha \mathcal{L}_F(\theta_T, X_F, X_R) + (1 - \alpha) \mathcal{L}_R(\theta_T, X_R, \theta_B)$ 
11:   $\theta_T \leftarrow \theta_T - \eta \nabla \mathcal{L}$ 
12: end for
13: Return  $f_{\theta_T}$ 

```

these images. When we consider the entire distribution, we are not concerned with the NLL of each image, but rather the entire distribution as a whole. Thus, we compare the NLL distribution of the original model $-\log p_X(\mathcal{D}_R; \theta_B)$ to that of the tamed model $-\log p_X(\mathcal{D}_R; \theta_T)$. The closer these distributions are, the less impact our procedure had on the images that we did not intend to forget. We use the *KL divergence* [33] between these distributions to measure their proximity. We use both the forward and reverse KL divergence, denoted as $\mathcal{L}_{KL_F}(\theta_T, \mathcal{D}_R, \theta_B)$ and $\mathcal{L}_{KL_R}(\theta_T, \mathcal{D}_R, \theta_B)$ respectively. Moreover, we also use the average negative log-likelihood loss $A(\mathcal{D}_R; \theta_T)$ (Eq. (5)), in order to preserve the NLL of the original model on \mathcal{D}_R . Our combined *remembering* loss is thus:

$$\begin{aligned} \mathcal{L}_R(\theta_T, \mathcal{D}_R, \theta_B) = & \gamma \cdot (\mathcal{L}_{KL_F}(\theta_T, \mathcal{D}_R, \theta_B) + \mathcal{L}_{KL_R}(\theta_T, \mathcal{D}_R, \theta_B)) \quad (12) \\ & + (1 - \gamma) \cdot A(\mathcal{D}_R; \theta_T), \end{aligned}$$

where γ is a hyperparameter that controls the ratio between the original task and the explicit distribution proximity loss. Notice that as \mathcal{D}_R can represent a distribution that is different than the original task (in case \mathcal{D}_R is not the training set used to train θ_B), the loss acts in line with this distribution. The “closer” \mathcal{D}_R is to the training set, the higher the preservation of θ_B image space. Our total objective is a weighted combination of the forget and remember losses:

$$\theta_T = \operatorname{argmin}_{\theta} \left\{ \alpha \cdot \mathcal{L}_F(\theta, \mathcal{D}_F, \mathcal{D}_R) + (1 - \alpha) (\mathcal{L}_R(\theta, \mathcal{D}_R, \theta_B)) \right\}. \quad (13)$$

We use SGD [2] optimization techniques to satisfy the equation, stopping the process when the term in Eq. (9) is satisfied. A summary of our method can be seen in Alg. 1.

4. Experiments

The experiments demonstrate reduction of the probability of generating images of a specific person, a set of people, and people possessing specific attributes. Our method can also be applied in the opposite direction, increasing the probability of image generation of certain groups in the population, to debias a model.

In our experiments, the base model f_{θ_B} is Glow [28] trained on 128×128 images from the FFHQ [26] dataset and the CelebA [35] training set. The training was done for 590K iterations for a total of 316.3 hours. Full technical details can be found in Appx. B. To improve our method’s runtime, we compute the parameters of the remember batch NLL distribution (see Line 5 in Alg. 1) every 10 iterations. Unless stated otherwise, when we compare NLL of different models, it is done by randomly sampling 10,000 images. In our analysis below, we focus on the effect on the forget set \mathcal{D}_F , as our method almost perfectly preserves the remember set \mathcal{D}_R (see Appx. A).

4.1. Taming an identity

First, we examine the ability to reduce the generation probability of a person’s images. This corresponds to many applications, *e.g.*, taming a pre-trained generative model that produces images that violate someone’s privacy.

In this experiment, we have access to \mathcal{D} , the training set used to train the given model. We wish to tame the model in such a way that images containing a specific identity will not be generated by the model, or at least to reduce this probability as we see fit. These images, denoted as \mathcal{D}_F , are a part of the training set, *i.e.* $\mathcal{D}_F \subset \mathcal{D}$. Therefore, the remember set in this case is defined as $\mathcal{D}_R := \mathcal{D} \setminus \mathcal{D}_F$. We run experiments with different sizes of \mathcal{D}_F , using the same hyperparameters used to train the original flow. We run the experiments until all the images that we wish to forget, \mathcal{D}_F , have a generation likelihood inside the error bound around the threshold (see Eq. (9)).

To quantify the results, we use the likelihood quantile $q(\cdot)$ (see Eq. (11)), generalizing it to all the examples in \mathcal{D}_F :

$$q(\mathcal{D}_F; \mathcal{D}_R; \theta_T) = 1 - \frac{1}{|\mathcal{D}_F|} \sum_{x \in \mathcal{D}_F} F_{\mu_R, \sigma_R}(-\log p_X(x; \theta_T)). \quad (14)$$

We report in Tab. 1 both the running time of the experiment and the likelihood of \mathcal{D}_F . Notice that the experiment was terminated only when the criteria in Eq. (9) was met, meaning all images in the forget set are within the error bound range. The NLL is transformed to quantile probability w.r.t. the NLL distribution of \mathcal{D}_R (see Eq. (11)). For example, the first line of the table shows that for an image in the bottom 0.25 quantile (compared to the likelihood of images in \mathcal{D}_R), after taming the same image is now in the bottom $2.15e-5$ quantile, significantly less likely.

# Images	Forget set \mathcal{D}_F		Forget reference set \mathcal{D}'_F		Remember set \mathcal{D}_R		T[min]	T[%]
	Base (θ_B)	Tamed (θ_T)	Base (θ_B)	Tamed (θ_T)	Base (θ_B)	Tamed (θ_T)		
1	0.25	2.15e-7	0.48	0.34	0.51	0.51	3.7	0.02%
4	0.57	7.4e-6	0.45	0.34	0.51	0.51	12.3	0.06%
8	0.49	9.3e-6	0.46	0.3	0.51	0.5	17.2	0.09%
15	0.53	1.7e-5	0.4	0.24	0.51	0.51	27.8	0.15%

Table 1. **Forget an identity from the training set.** Likelihood quantile of forget samples before and after our process, for different sizes of \mathcal{D}_F . \mathcal{D}'_F is a holdout set from the same identity as \mathcal{D}_F . \mathcal{D}_R results are based on a random sample of 100 images. T[min] is the time taken to run this experiment in minutes. T[%] is the relative percentage difference between the experiment’s runtime and the base model’s total training time. Each row is an average of 5 experiments. The table shows that we are able to forget an identity quickly (see T[%] column), without affecting the rest of the people in the dataset (results on \mathcal{D}_R are not affected).



Figure 3. **Visual generation evaluation.** Generated samples from the base model, θ_B , and a model tamed to forget 15 images of an identity in the training set, θ_T . These models achieve a similar FID score [21] of 140.89 and 141.63 respectively. The even columns contain images produced by the tamed model θ_T , and the odd columns by the base θ_B .

Tab. 1 shows we are able to reach the desired threshold quickly, with a runtime that does not exceed 0.15% of base model’s training time. We also see that the NLL of other unseen images of the same identity, \mathcal{D}'_F , increases as the number of images of that identity, $|\mathcal{D}_F|$, that are involved in the process grows. This is a surprising result, as we do not force resemblance of images during our process, suggesting that by forcing the model to deviate from certain images, it learns to generalize to other same identity images.

To investigate whether the quality of image generation is preserved by using our method, we present in Fig. 3 generated images before and after applying our method. The figure shows that we do not hurt the quality of image generation, as the faces generated by the model we tamed are indistinguishable from the faces generated by the base model. Appx. A contains results for a slightly different setup, where the identities we forget are not from the training set, *i.e.* $\mathcal{D}_F \not\subset \mathcal{D}$.

4.2. Taming an attribute

Next, we zoom out from the local effect on a small number of images, to a broader aspect of change. We show that our method can be applied even when the desired change is more general, *e.g.* reducing the probability of generated images that contain inappropriate content.

In this experiment we have access to \mathcal{D} , the model’s training set. We wish to forget an attribute common to

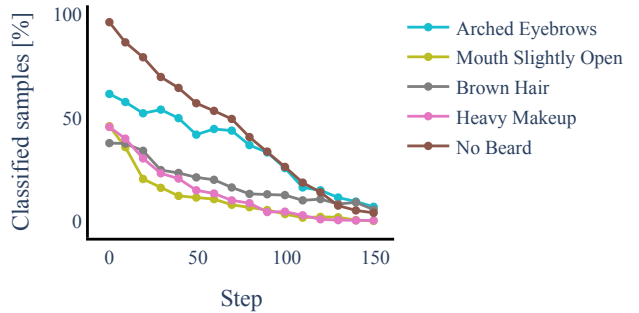


Figure 4. **Taming attributes.** Results for forgetting attributes as explained in Sec. 4.2, meaning forgetting a more global property and not a specific small number of images. X-axis: number of steps of our applied method; Y-axis: fraction of random samples (out of 512) that are classified as holding the corresponding property. Each model was altered to reduce the probability of a different property, taken from the labels of CelebA.

many images in the training set, *e.g.* wearing glasses or smiling. Thus, we use a classifier for that property, denoted as $C : \mathcal{X} \rightarrow \{0, 1\}$ to define the remember and forget sets: $\mathcal{D}_F = \{x \in \mathcal{D} \mid C(x) = 1\}$, $\mathcal{D}_R = \mathcal{D} \setminus \mathcal{D}_F$. We train a classifier $C(\cdot)$ on CelebA.

As we wish to reduce the probability of generating images with some property, evaluating this experiment is straightforward, by passing random samples from the prior distribution through the normalizing flow, and classifying the output images. Our method alters the model, in order to reduce the number of outputs classified as possessing the relevant attribute. This approach can be used to debias a model, *e.g.* a model that generates images of a certain group of the population with high probability (high to the point of over representing it), one can use our method in order to reduce that probability.

The results are shown in Fig. 4, showing we are able to tune a model to reduce the sampling rate of an attribute. This process takes roughly 4 times more than the maximal time shown in the previous experiment (see Tab. 1), still less than 1% of the time to initially train the base model θ_B .

This method can also be used in the opposite direction, to increase the number of generated samples possessing the

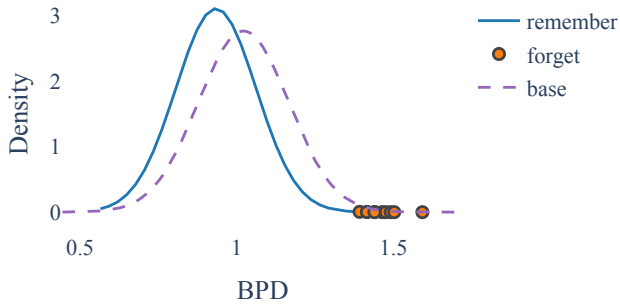


Figure 5. **Forget without training data access.** When the remember images (solid) are different than the training data of the base model θ_B (dashed), we are still able to forget images w.r.t. to the NLL of the remember images (orange dots). the x-axis is NLL in units of bits per dimension (BPD [38]), meaning lower is more likely.

chosen attribute. This means that in this case, instead of forgetting a group of images, we do the opposite and enhance the representation of these images in the output space. Appx. C includes such examples used for model de-biasing, along with generated examples showing the effect of the different attribute changes.

4.3. Taming without train set

Next, we examine situations where we do not have access to the model’s training data. An example of such a scenario can be a company that releases a generative model to the public, without the data on which it was trained. Entities using this model might want to alter the model w.r.t. different data, while maintaining the model’s performance.

In this experiment, the setup is similar to the one in Sec. 4.1, except that \mathcal{D} is not the training set of the model, but a set of images that are disjoint to the training data. We sourced images from Fairface [24], opting for faces of children in the age gap of 3–9 years, according to their labels. We chose these images for a distribution of natural faces that is different from CelebA’s, as it consists of fewer young faces. We experimented with a set of 1000 images as \mathcal{D}_R , and 10 images as \mathcal{D}_F .

Results are shown in Fig. 5. The graph shows the NLL distributions, in units of bits per dimension (BPD), of the “remember” images \mathcal{D}_R (solid) against the base model on the training data \mathcal{D} (dashed). The distance between the two Gaussians demonstrates the difference in the NLL distribution of \mathcal{D} and \mathcal{D}_R . The orange dots mark the images to be forgotten \mathcal{D}_F , which are “pushed” to the tail of the distribution and have very low probability of being sampled.

Impact of size of \mathcal{D}_F : In the following experiment we evaluate the impact the number of images to be forgotten has on our method (Fig. 6).

As can be seen, when the size of \mathcal{D}_F is small (i.e., $|\mathcal{D}_F| < 40$) the model successfully forgets them (their likelihood quantile is near zero). When $|\mathcal{D}_F| > 40$, the model

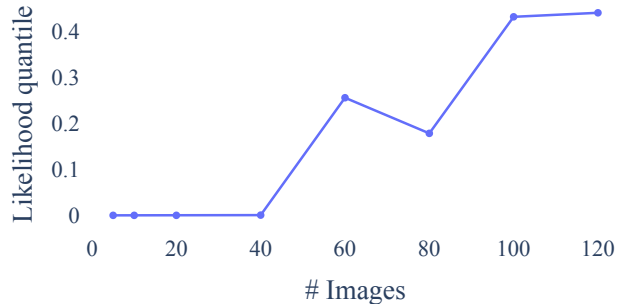


Figure 6. **Taming success against number of samples.** The plot shows the likelihood quantile of different models without any access to the training data. \mathcal{D}_R contains 1000 images out of the base model’s training set. Each model is tamed to forget a different number of images (the x-axis). We see that when \mathcal{D}_F is small, taming can yield a big likelihood reduction, while on a lot of images the average difference drops.

can no longer forget those images (while still remembering the images in \mathcal{D}_R).

We conclude that for a small number of images, roughly 1–40, our method can reside these images a significant distance away from the base log-likelihood distribution. For more images, this distance becomes smaller, but the overall generated distribution is still affected by our process, as shown in the experiment of forgetting attributes in Sec. 4.1. Appx. C contains an evaluation of images generated by these models.

5. Ablation study

This study demonstrates the importance of different parts of our method. This is done by removing some parts of our loss term, according to the objective term in Eq. (13). The models were fine-tuned on top of the base model, in order to forget 15 images of an identity from CelebA. We now evaluate the results qualitatively and quantitatively.

Qualitative comparison. To compare the different models qualitatively, we compare the quality of images generated by them. We randomly sampled two latent vectors from the prior distribution, and passed them through the different models. Fig. 7 shows the results of this study.

Without any loss that preserves the knowledge of the original objective (the \mathcal{L}_R loss), the quality of the generated images is significantly worse. Furthermore, we see that the reverse KL divergence loss, \mathcal{L}_{KL_R} , is vital to produce images with high quality. There are some parts of the total loss term that seem to have a lower effect on the generation quality (the 2–4 columns on the right in Fig. 7), but only when using the full loss objective, we get a model that preserves the original images with high quality. This is shown clearly in the figure as only the rightmost column preserves the original generated images. This result suggests that using our method, we can preserve the behavior in the latent space and apply changes very specifically. Since

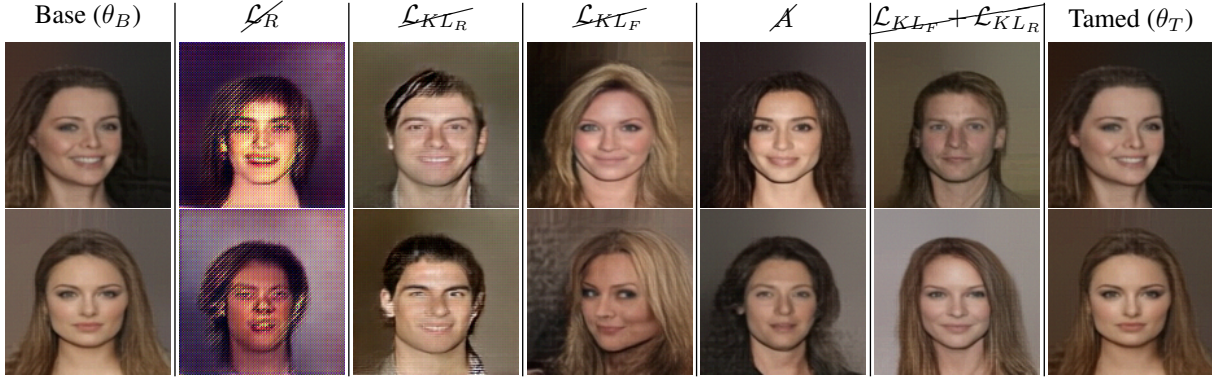


Figure 7. **Qualitative ablation comparison.** For a fixed couple of latent vectors drawn from the tractable prior distribution, the shown images were acquired by passing the latents through different normalizing flows. Each column represents the output of a different model. Each middle column represents a model that was trained while eliminating a different part of the loss, *e.g.* \mathcal{L}_R uses the entire loss term apart from the remember loss \mathcal{L}_R . The different loss components are presented in Eqs. (12) and (13).

Model	BPD mean \downarrow	FID \downarrow	Likelihood quantile
Base (θ_B)	1.021	140.89	-
\mathcal{L}_R	25.64	181.26	0.34
\mathcal{L}_{KL_R}	2.254	110.34	0.73
\mathcal{L}_{KL_F}	1.072	121.45	2.45e-5
\mathcal{A}	1.025	141.99	1.02e-5
$\mathcal{L}_{KL_F} + \mathcal{L}_{KL_R}$	1.028	143.16	8.53e-6
Tamed (θ_T)	1.02	141.63	2.35e-5

Table 2. **Quantitative ablation study.** Comparison of the NLL (in BPD [38] units), FID and likelihood quantile. For the models name notation see Fig. 7 and Eqs. (12) and (13).

there are many methods that utilize different properties of latent spaces in generative models [44, 45], this is of value, and we aim to preserve these properties.

Quantitative comparison. Tab. 2 shows a comparison of the different ablated models. A full comparison can be found in the supplementary material. We see that regarding the NLL (measured in BPD in the table), when we use a KL divergence loss, reverse KL divergence is crucial to ensure a high likelihood of the training data, as it is suited for data generation tasks. When omitting \mathcal{L}_R the FID [21] score grows, and the forgetting objective (the likelihood quantile column) grows as well. The growth in FID score means we drift from the original data, and the large likelihood score means the model does not forget that data it was supposed to forget. Omitting the \mathcal{L}_{KL_R} term maintains similarity with the original data (low FID), but fails to forget (again, the likelihood is quite high).

5.1. Limitations

Our method is demonstrated on normalizing flows, and we do not demonstrate it on explicit generative models at all. Moreover, our precise evaluation of forgetting data samples is based on the assumption of normality on the model's

NLL training set. Although we do offer a qualitative measurement using a normality test as mentioned in Sec. 3.3, models that do not align with this assumption will find the threshold we use less powerful and accurate.

6. Ethical considerations

As generative models such as GANs [15] and diffusion models [22] have gained immense popularity in recent years, the wider public interest in these models increases and important issues arise with respect to the generation of hateful, fake, explicit and biased content. Many establishments that train these kind of models are concerned about these potential risks, and choose to opt out of their public release. In our work, we try to proceed in a direction that can help bound these malicious applications, and help towards their mitigation. Although our method can be used in a positive manner, unfortunately, it can also be used in the opposite direction, *e.g.* increasing a known bias of a model instead of debiasing it. We are aware of these potential risks, and suggest that individuals using this work will do so carefully, realizing that it can be exploited in the wrong hands.

7. Conclusion

In this work, we proposed an approach towards taming generative models, controlling their output by increasing or decreasing the probability of generation for selected data. We demonstrated different aspects of our method on normalizing flows, showing it can be applied fast, evaluated easily, with minimal collateral damage to the model, in order to support the high scale usage of these models. We hope that our work can serve as a stepping stone for future research on controlling different types of generative models, enabling better supervision of their output.

References

[1] David Ahmedt-Aristizabal, Mohammad Ali Armin, Simon Denman, Clinton Fookes, and Lars Petersson. Graph-based deep learning for medical diagnosis and analysis: past, present and future. *Sensors*, 21(14):4758, 2021. [2](#)

[2] Shun-ichi Amari. Backpropagation and stochastic gradient descent method. *Neurocomputing*, 5(4-5):185–196, 1993. [4](#), [5](#)

[3] Dmitrii Babaev, Maxim Savchenko, Alexander Tuzhilin, and Dmitrii Umerenkov. Et-rnn: Applying deep learning to credit loan applications. In *Proceedings of the 25th ACM SIGKDD international conference on knowledge discovery & data mining*, pages 2183–2190, 2019. [2](#)

[4] Sina Baharlouei, Maher Nouiehed, Ahmad Beirami, and Meisam Razaviyayn. R\’enyi fair inference. *arXiv preprint arXiv:1906.12005*, 2019. [2](#)

[5] David Bau, Steven Liu, Tongzhou Wang, Jun-Yan Zhu, and Antonio Torralba. Rewriting a deep generative model. In *European conference on computer vision*, pages 351–369. Springer, 2020. [2](#)

[6] Yoshua Bengio, Eric Laufer, Guillaume Alain, and Jason Yosinski. Deep generative stochastic networks trainable by backprop. In *International Conference on Machine Learning*, pages 226–234. PMLR, 2014. [2](#)

[7] Lucas Bouroule, Varun Chandrasekaran, Christopher A Choquette-Choo, Hengrui Jia, Adelin Travers, Baiwu Zhang, David Lie, and Nicolas Papernot. Machine unlearning. In *2021 IEEE Symposium on Security and Privacy (SP)*, pages 141–159. IEEE, 2021. [3](#)

[8] Nicholas Carlini, Florian Tram\`er, Eric Wallace, Matthew Jagielski, Ariel Herbert-Voss, Katherine Lee, Adam Roberts, Tom Brown, Dawn Song, \U00c3lfar Erlingsson, Alina Oprea, and Colin Raffel. Extracting training data from large language models. In *30th USENIX Security Symposium (USENIX Security 21)*, pages 2633–2650. USENIX Association, Aug. 2021. [3](#)

[9] Min Chen, Zhikun Zhang, Tianhao Wang, Michael Backes, Matthias Humbert, and Yang Zhang. When machine unlearning jeopardizes privacy. In *ACM SIGSAC Conference on Computer and Communications Security (CCS)*, 2021. [3](#)

[10] Anton Cherepkov, Andrey Voynov, and Artem Babenko. Navigating the gan parameter space for semantic image editing. In *Proceedings of the IEEE/CVF conference on computer vision and pattern recognition*, pages 3671–3680, 2021. [2](#)

[11] The Conversation. <https://theconversation.com/the-use-of-deepfakes-can-sow-doubt-creating-confusion-and-distrust-in-viewers-182108>. [1](#)

[12] Laurent Dinh, David Krueger, and Yoshua Bengio. NICE: Non-linear Independent Components Estimation, Apr. 2015. Number: arXiv:1410.8516 arXiv:1410.8516 [cs]. [1](#), [3](#)

[13] Laurent Dinh, Jascha Sohl-Dickstein, and Samy Bengio. Density estimation using Real NVP, Feb. 2017. Number: arXiv:1605.08803 arXiv:1605.08803 [cs, stat]. [1](#), [2](#), [3](#)

[14] Aditya Golatkar, Alessandro Achille, and Stefano Soatto. Eternal Sunshine of the Spotless Net: Selective Forgetting in Deep Networks. In *2020 IEEE/CVF Conference on Computer Vision and Pattern Recognition (CVPR)*, pages 9301–9309, Seattle, WA, USA, June 2020. IEEE. [3](#)

[15] Ian Goodfellow, Jean Pouget-Abadie, Mehdi Mirza, Bing Xu, David Warde-Farley, Sherjil Ozair, Aaron Courville, and Yoshua Bengio. Generative adversarial nets. *Advances in neural information processing systems*, 27, 2014. [1](#), [2](#), [8](#)

[16] Ian J Goodfellow, Mehdi Mirza, Da Xiao, Aaron Courville, and Yoshua Bengio. An empirical investigation of catastrophic forgetting in gradient-based neural networks. *arXiv preprint arXiv:1312.6211*, 2013. [3](#)

[17] Chuan Guo, Tom Goldstein, Awini Hannun, and Laurens van der Maaten. Certified Data Removal from Machine Learning Models, Aug. 2020. arXiv:1911.03030 [cs, stat]. [3](#)

[18] Niv Haim, Gal Vardi, Gilad Yehudai, Ohad Shamir, and Michal Irani. Reconstructing training data from trained neural networks. *arXiv preprint arXiv:2206.07758*, 2022. [3](#)

[19] Jun Han and Claudio Moraga. The influence of the sigmoid function parameters on the speed of backpropagation learning. In *International workshop on artificial neural networks*, pages 195–201. Springer, 1995. [4](#)

[20] GM Harshvardhan, Mahendra Kumar Gourisaria, Manjusha Pandey, and Siddharth Swarup Rautaray. A comprehensive survey and analysis of generative models in machine learning. *Computer Science Review*, 38:100285, 2020. [1](#)

[21] Martin Heusel, Hubert Ramsauer, Thomas Unterthiner, Bernhard Nessler, and Sepp Hochreiter. Gans trained by a two time-scale update rule converge to a local nash equilibrium. In I. Guyon, U. Von Luxburg, S. Bengio, H. Wallach, R. Fergus, S. Vishwanathan, and R. Garnett, editors, *Advances in Neural Information Processing Systems*, volume 30. Curran Associates, Inc., 2017. [6](#), [8](#)

[22] Jonathan Ho, Ajay Jain, and Pieter Abbeel. Denoising diffusion probabilistic models. *Advances in Neural Information Processing Systems*, 33:6840–6851, 2020. [1](#), [8](#)

[23] Jonathan Ho, Ajay Jain, and Pieter Abbeel. Denoising diffusion probabilistic models. In H. Larochelle, M. Ranzato, R. Hadsell, M.F. Balcan, and H. Lin, editors, *Advances in Neural Information Processing Systems*, volume 33, pages 6840–6851. Curran Associates, Inc., 2020. [2](#)

[24] Kimmo K\"arkk\"ainen and Jungseock Joo. Fairface: Face attribute dataset for balanced race, gender, and age. *arXiv preprint arXiv:1908.04913*, 2019. [7](#), [18](#)

[25] Tero Karras, Timo Aila, Samuli Laine, and Jaakko Lehtinen. Progressive growing of gans for improved quality, stability, and variation. *arXiv preprint arXiv:1710.10196*, 2017. [3](#)

[26] Tero Karras, Samuli Laine, and Timo Aila. A style-based generator architecture for generative adversarial networks. In *Proceedings of the IEEE/CVF Conference on Computer Vision and Pattern Recognition (CVPR)*, June 2019. [3](#), [5](#), [11](#)

[27] Diederik P. Kingma and Jimmy Ba. Adam: A method for stochastic optimization. In Yoshua Bengio and Yann LeCun, editors, *3rd International Conference on Learning Representations, ICLR 2015, San Diego, CA, USA, May 7-9, 2015, Conference Track Proceedings*, 2015. [11](#)

[28] Diederik P. Kingma and Prafulla Dhariwal. Glow: Generative Flow with Invertible 1x1 Convolutions, July 2018. Number: arXiv:1807.03039 arXiv:1807.03039 [cs, stat]. [1](#), [3](#), [5](#), [11](#)

[29] Diederik P Kingma and Max Welling. Stochastic gradient vb and the variational auto-encoder. In *Second International Conference on Learning Representations, ICLR*, volume 19, page 121, 2014. [1](#), [2](#)

[30] James Kirkpatrick, Razvan Pascanu, Neil Rabinowitz, Joel Veness, Guillaume Desjardins, Andrei A. Rusu, Kieran Milan, John Quan, Tiago Ramalho, Agnieszka Grabska-Barwinska, Demis Hassabis, Claudia Clopath, Dharshan Kumaran, and Raia Hadsell. Overcoming catastrophic forgetting in neural networks. *Proc. Natl. Acad. Sci. U.S.A.*, 114(13):3521–3526, Mar. 2017. arXiv:1612.00796 [cs, stat]. [3](#)

[31] Ivan Kobyzev, Simon JD Prince, and Marcus A Brubaker. Normalizing flows: An introduction and review of current methods. *IEEE transactions on pattern analysis and machine intelligence*, 43(11):3964–3979, 2020. [1](#), [3](#)

[32] Zhifeng Kong and Kamalika Chaudhuri. Forgetting data from pre-trained gans. *arXiv preprint arXiv:2206.14389*, 2022. [2](#)

[33] Solomon Kullback and Richard A Leibler. On information and sufficiency. *The annals of mathematical statistics*, 22(1):79–86, 1951. [5](#)

[34] Lucien Le Cam. Maximum likelihood: an introduction. *International Statistical Review/Revue Internationale de Statistique*, pages 153–171, 1990. [2](#)

[35] Ziwei Liu, Ping Luo, Xiaogang Wang, and Xiaou Tang. Deep learning face attributes in the wild. In *Proceedings of International Conference on Computer Vision (ICCV)*, December 2015. [1](#), [5](#), [11](#)

[36] F. J. Massey. The Kolmogorov-Smirnov test for goodness of fit. *Journal of the American Statistical Association*, 46(253):68–78, 1951. [4](#), [11](#)

[37] Vinod Nair and Geoffrey E Hinton. Rectified linear units improve restricted boltzmann machines. In *Icml*, 2010. [1](#), [2](#)

[38] George Papamakarios, Theo Pavlakou, and Iain Murray. Masked autoregressive flow for density estimation. *Advances in neural information processing systems*, 30, 2017. [7](#), [8](#)

[39] The Washington Post. <https://www.washingtonpost.com/nation/2021/03/13/cheer-mom-deepfake-teammates/>. [1](#)

[40] Vikram V Ramaswamy, Sunnie SY Kim, and Olga Russakovsky. Fair attribute classification through latent space de-biasing. In *Proceedings of the IEEE/CVF conference on computer vision and pattern recognition*, pages 9301–9310, 2021. [2](#)

[41] General Data Protection Regulation. <https://gdpr-info.eu/>. [1](#), [3](#)

[42] Danilo Rezende and Shakir Mohamed. Variational inference with normalizing flows. In *International conference on machine learning*, pages 1530–1538. PMLR, 2015. [1](#), [2](#)

[43] Danilo Rezende and Shakir Mohamed. Variational inference with normalizing flows. In *International conference on machine learning*, pages 1530–1538. PMLR, 2015. [3](#)

[44] Yujun Shen, Jinjin Gu, Xiaou Tang, and Bolei Zhou. Interpreting the latent space of gans for semantic face editing. In *Proceedings of the IEEE/CVF Conference on Computer Vision and Pattern Recognition (CVPR)*, June 2020. [8](#)

[45] Alon Shoshan, Nadav Bhotker, Igor Kviatkovsky, and Gerard Medioni. Gan-control: Explicitly controllable gans. In *Proceedings of the IEEE/CVF International Conference on Computer Vision*, pages 14083–14093, 2021. [8](#)

[46] Lucas Theis, Aäron van den Oord, and Matthias Bethge. A note on the evaluation of generative models. *arXiv preprint arXiv:1511.01844*, 2015. [11](#)

[47] Harri Valpola, Xavier Giannakopoulos, Antti Honkela, and Juha Karhunen. Nonlinear independent component analysis using ensemble learning: Experiments and discussion. In *Proc. Int. Workshop on Independent Component Analysis and Blind Signal Separation (ICA2000)*, pages 351–356, 2000. [2](#)

[48] Aäron van den Oord and Nal Kalchbrenner. Pixel rnn. In *ICML*, 2016. [2](#)

[49] Sheng-Yu Wang, David Bau, and Jun-Yan Zhu. Rewriting geometric rules of a gan. *ACM Transactions on Graphics (TOG)*, 41(4):1–16, 2022. [2](#)

[50] WIRED. <https://www.wired.com/story/zelensky-deepfake-facebook-twitter-playbook/>. [1](#)

Appendices

In the next sections we provide additional results, along with additional visualizations and details, further demonstrating our method’s applications.

A. Results

In this section, we discuss additional results associated with experiments from our paper. We show:

1. Results evaluating our method on the remember set \mathcal{D}_R .
2. An extension of the experiment concerning forgetting an identity, to an unknown identity that is outside the training set.
3. A full comparison of the experiment for forgetting without any access to the training set.
4. Evaluation of the effect that training set size has on our method’s running time.
5. An extension of our ablation study, comparing the preservation of the training set distribution.

We first discuss how our method preserves the NLL distribution of the remember set \mathcal{D}_R . In Sec. 4, we showed results focusing on the forget set \mathcal{D}_F . We now show results, focusing on \mathcal{D}_R . This is demonstrated by showing this distribution before and after taming, as can be seen in Fig. A.1. The figure visualizes the differences between the normalized density histogram of the base model (θ_B) and the tamed model (θ_T), along with normal estimation of these distributions, denoted as $\hat{\theta}_B$ and $\hat{\theta}_T$ respectively, on the training set and an unseen set. As we trained θ_B on the training set of CelebA [35], we used the validation set of CelebA as an unseen set on all upcoming demonstrations, unless specified otherwise. The distribution pairs in Fig. A.1 are all similar, indicating that we successfully forget the target(s), without heavily impacting the rest of the distribution.

Next, we discuss the experiment of forgetting an identity, as shown in Sec. 4.1. In Tab. A.1 we present the results for an experiment of forgetting an identity outside the training set, using an identity from an unseen data set. We see the results are similar to the ones in Tab. 1 — we are still able to “forget”, with similar runtime.

In Fig. A.2 we show a full comparison for the experiment on forgetting without the training set, shown in Fig. 5. We see that regarding the NLL distribution of the tamed model θ_T , while there is a degradation, it is still close to the distribution of the base model θ_B on the same data.

Now we turn to inspect whether the time to forget an identity depends on the number of images the model was

trained on. To do so, we trained an additional base model just on CelebA. This model was trained on 162,770 images, while the original one, trained additionally on FFHQ [26], was trained on 232,770. For both models, training stopped with the same performance (in NLL) on CelebA’s training set. In Tab. A.2, we compare the running time of these models, and see that in time that is relative to the model’s training time, taming a model that was trained on CelebA only takes longer, but this time is still relatively small, less than 1% of the total training time of the model.

As discussed in Sec. 5, in Fig. A.3 we compare the distribution of NLL values on the training set of the base model, for different ablated models. Some models are not shown in the figure, as they have a distribution that is visually indistinguishable from the shown distributions of the base and tamed models. The figure shows that without using the forward KL divergence loss (\mathcal{L}_{KL_F}), the distribution is worse, but it’s also more “narrow”, fitting the mode-seeking behavior of the reverse KL divergence. On the contrary, without the reverse KL divergence (\mathcal{L}_{KL_R}), which is known to be important for generative tasks, the performance is bad, and fits the mean-seeking behavior of forward kl divergence, attempting to cover more regions.

B. Additional details

Next, we elaborate on technical details regarding the implementation of our method, as explained in Sec. 4. We trained a Glow [28] base model to produce RGB images with dimensions 128×128 . The training was done for 590K iterations with batch size of 32, for a total of 316.3 hours, using 4 12GB Titan Xp GPUs. The model has 4 blocks of 32 flows, each consisting of activation normalization layers, 1×1 LU decomposed convolution and additive coupling. The model is trained using an Adam [27] optimizer with learning rate $5 \cdot 10^{-5}$ and betas $(\beta_1, \beta_2) = (0.9, 0.999)$. Images are quantized to 5 bits and learned using the continuous dequantization process as done in previous work [28, 46]. For the forgetting process, we use a threshold of $\delta = 4$ and a bound of $\epsilon = 0.3$, along with hyperparameters $\alpha = 0.6$ and $\gamma = 0.6$, in all our experiments.

Now, we discuss the normality assumption as explained in Sec. 3.3. We assumed the NLL distribution of the base model on the training data is normal. To support this assumption, Fig. B.1 visually compares the distribution with a normal estimation, along with QQ-plots that further support this claim. We also performed a *Kolmogorov–Smirnov test* [36] and received a p-value of 0.95, 0.54 on 2000 random samples of CelebA’s training and validation sets, respectively. Thus, these results suggest that assuming a normal distribution is reasonable.

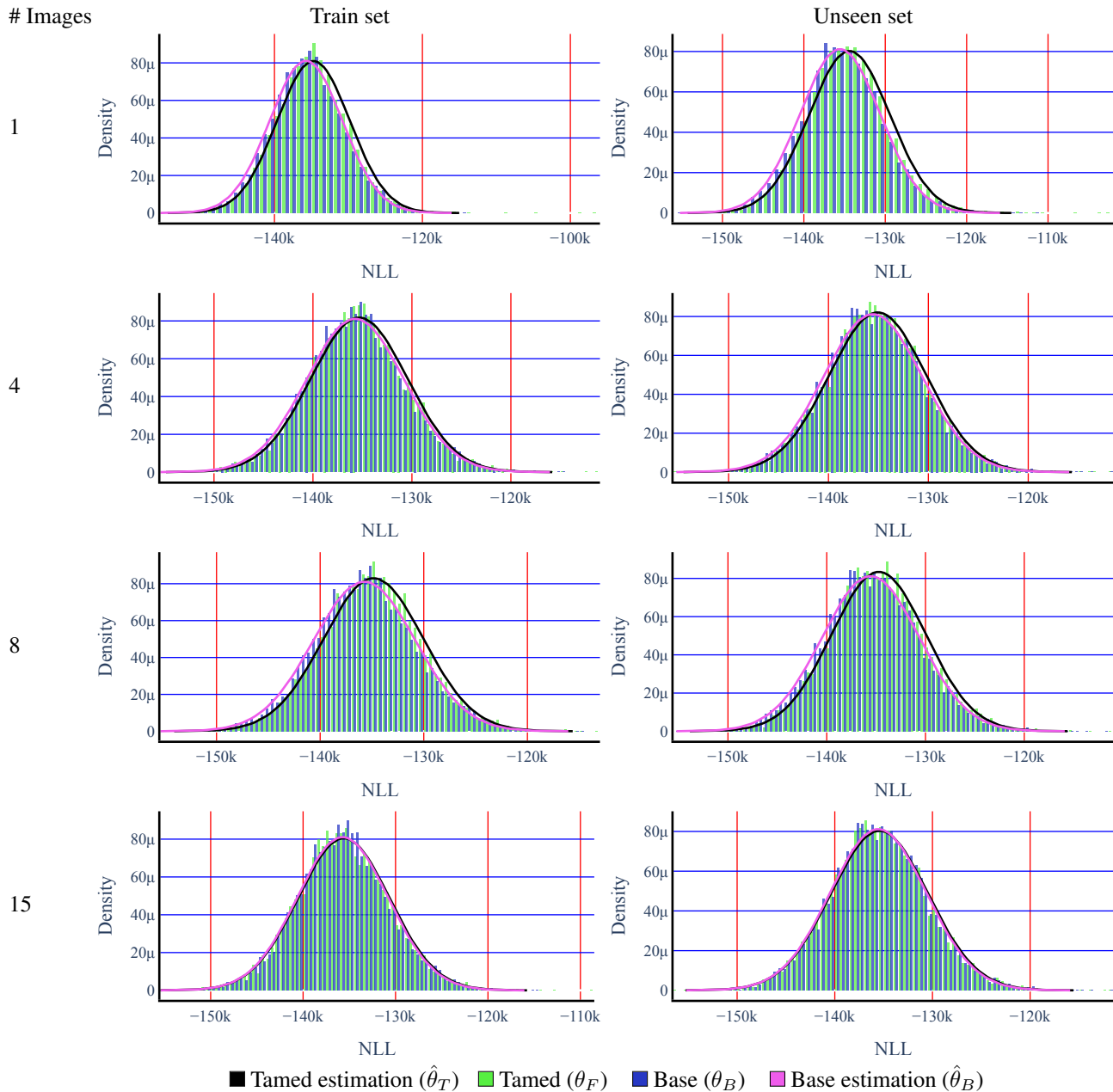


Figure A.1. Preserving the remember NLL distribution. Normalized density histogram and normal estimation of the NLL distribution on the base model training set, and a similar unseen set. The different plots correspond to models that were tamed to forget images of a specific identity, with a varying number of images. The graphs show that visually, the distributions are similar.

C. Visualizations

In this section we show different generated samples of tamed models from the different experiments in Sec. 4.

We begin with Fig. C.1, showing the generated images achieved from a model that was tamed to forget an attribute, specifically blond hair. We see the model outputs only images with black hair after this change. Figs. C.2 and C.3 Show how to tame a model in order to generate images with

some property with higher probability, specifically on people wearing glasses, and males. The desired sampling percentage can be controlled by the number of iterations of the process, *e.g.* in Fig. C.3 running for 210 iterations changes the model to generate only males (with high probability), while running for less iterations still generates females.

In Fig. C.4, we see the generated images when experimenting without any access to the training set, as the experiment in Sec. 4.3. When the remember set \mathcal{D}_R is very

# Images	Forget set \mathcal{D}_F		Forget reference set \mathcal{D}'_F		Remember set \mathcal{D}_R		T[min]	T[%]
	Base (θ_B)	Tamed (θ_T)	Base (θ_B)	Tamed (θ_T)	Base (θ_B)	Tamed (θ_T)		
1	0.3	1.73e-5	0.35	0.29	0.54	0.54	2.9	0.02%
4	0.37	1.39e-5	0.37	0.23	0.54	0.54	9.2	0.05%
8	0.42	1.22e-5	0.37	0.15	0.54	0.55	14.4	0.08%
15	0.48	5.41e-6	0.39	0.08	0.54	0.54	21.9	0.12%

Table A.1. **Forget an identity out of the training set.** Reported experiments as shown in Tab. 1, with the difference of performing the experiments on an identity outside the training set. Even when the identity we forget is not in the training set, we are able to forget its images quickly, as we see from the forget set \mathcal{D}_F tamed (θ_T) column.

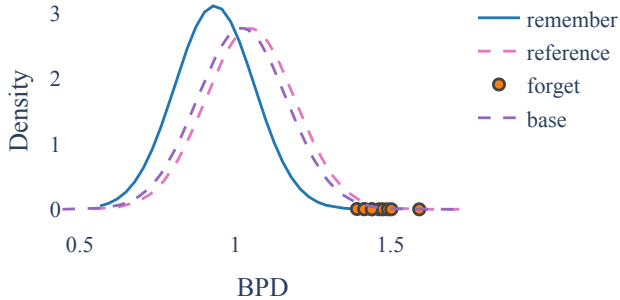


Figure A.2. **Forgetting without training data.** Full comparison of Fig. 5. Here we see not only the NLL distributions of θ_T on the remember set (solid), but also on the training distribution (dashed pink). The distribution of the base model θ_B on the training data (dashed purple) is close to the tamed model on the same data. We see the forget images (orange dots) are forgotten, reaching the desired threshold.

# Images	CelebA+FFHQ		CelebA	
	T[min]	T[%]	T[min]	T[%]
1	3.7	0.02%	3.0	0.03%
4	12.3	0.06%	8.3	0.08%
8	17.2	0.09%	14.5	0.14%
15	27.8	0.15%	27.9	0.27%

Table A.2. **Training size effect on running time.** A comparison of taming to forget images of an identity from the training set, for different amounts of forget images (*i.e.* $|\mathcal{D}_F|$). The two models differ in the training sets used to train them. T[min] is the time taken to run this experiment in minutes. T[%] is the experiment’s runtime vs. the base model’s total training time, in percents.

different from the original data, we see that while we do forget the desired image, we have a degradation in the generated image quality. When the remember set is closer to the training set, as in the validation set of CelebA, we see the generation quality remains high.

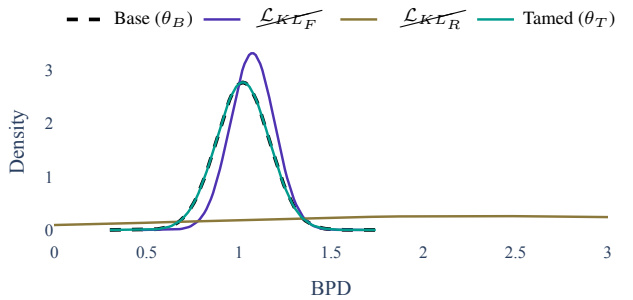


Figure A.3. **Ablation distribution comparison.** Comparison of the NLL distribution of models presented in Sec. 5. Notice how \mathcal{L}_{KL_R} and \mathcal{L}_{KL_F} do not preserve the base distribution well.

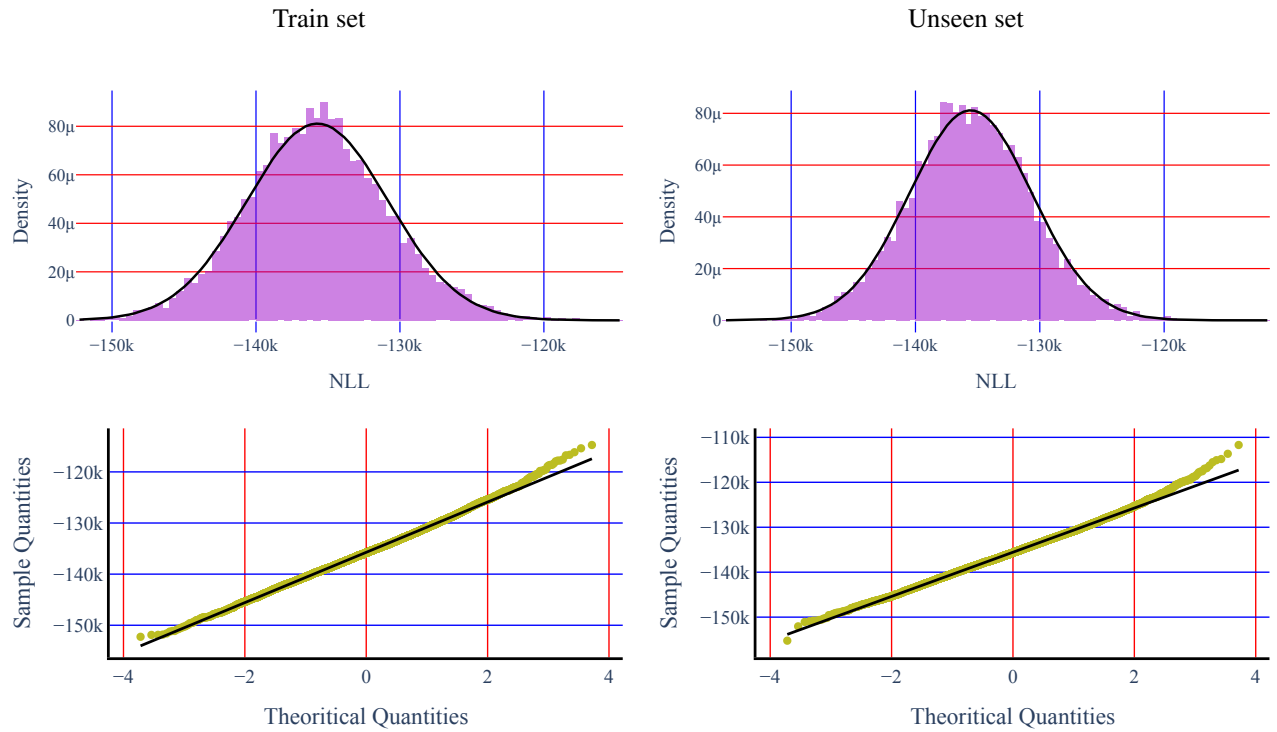


Figure B.1. **Base model (θ_B) NLL normal assumption.** For the base model’s training set (left) and a similar unseen set (right), we show a QQ-plot against normal distribution (lower row). We also show (upper row) the normalized density histogram (purple) and a Gaussian estimation (black line) of the distribution. We see visually that a normal distribution assumption fits this case.



Figure C.1. **Forget blond hair.** Images generated using a model that was tamed to “forget” blond hair, meaning to reduce the probability of generating images of people possessing blond hair.

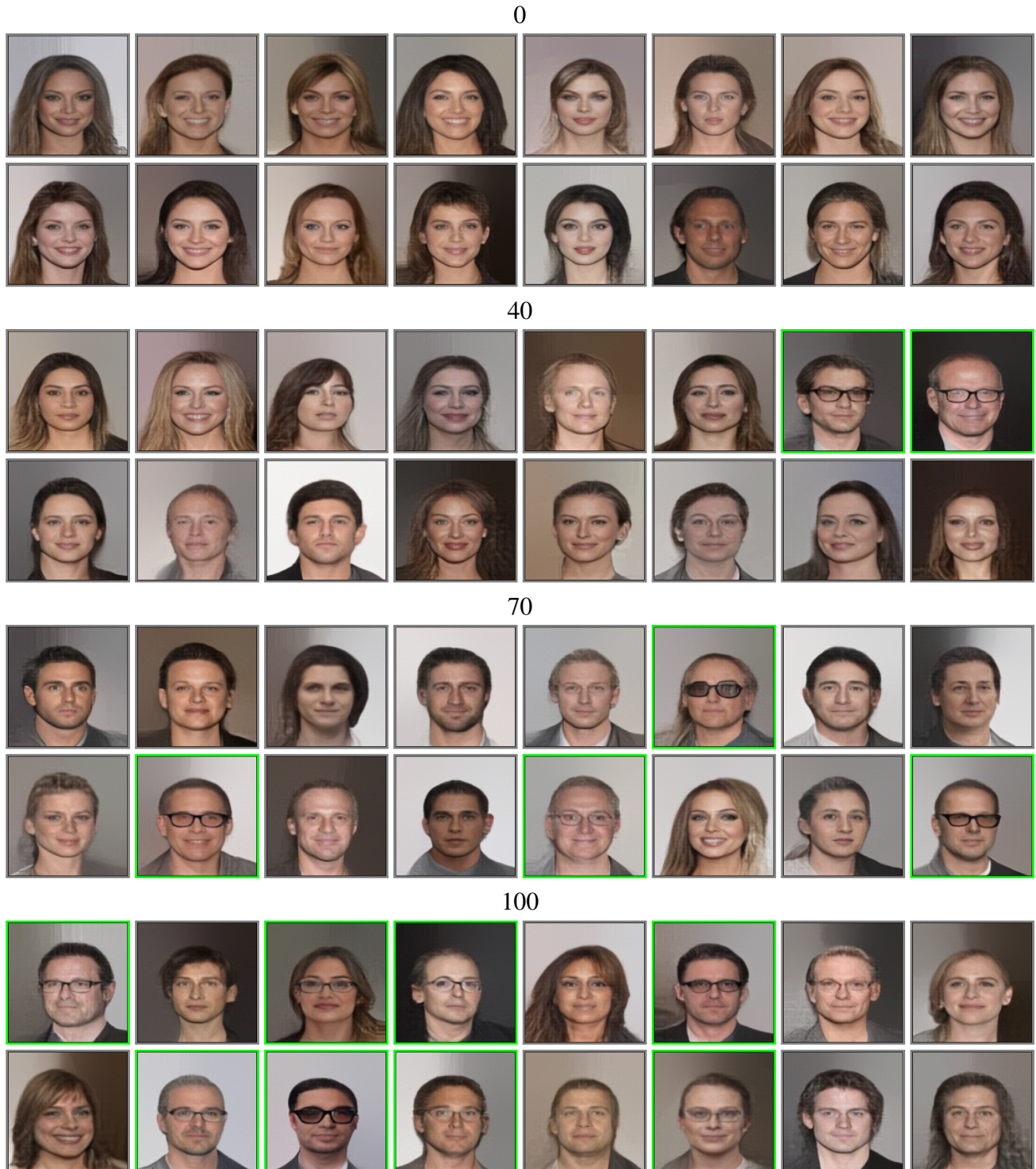
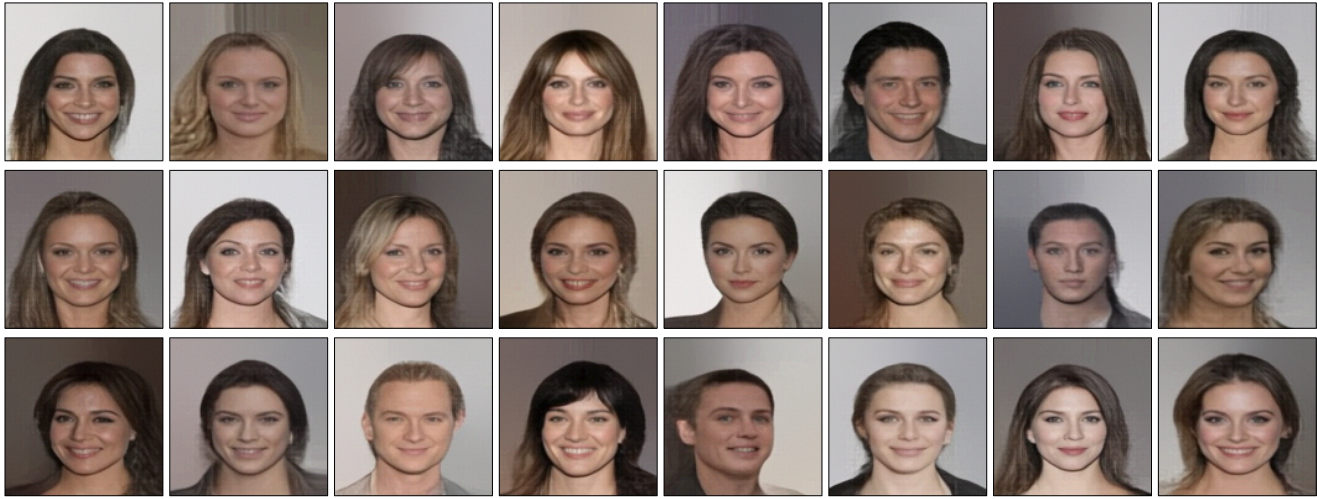
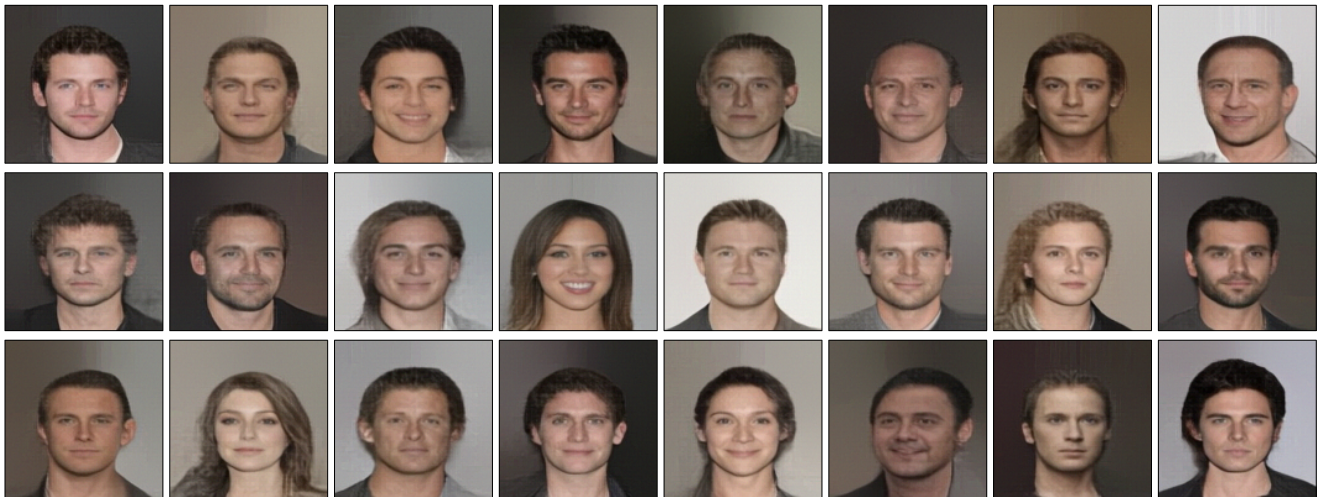


Figure C.2. **Increase glasses.** Images generated by a model tamed to increase the ratio of images of people wearing glasses. the numbers represent the number of iterations of our method. The images with a green frame are of people wearing glasses. We see that after 100 iterations most of the generated images are of people wearing glasses.

0



110



210



Figure C.3. **Increase Males.** The base model (θ_B) generates images of females with higher probability (0 iterations). Our method is used to tame a model to increase the generation probability of males, depending on the number of iterations we run our method (110, 210). We see that only after 210 iterations we are able to achieve a model that generates only images of males (with high probability).

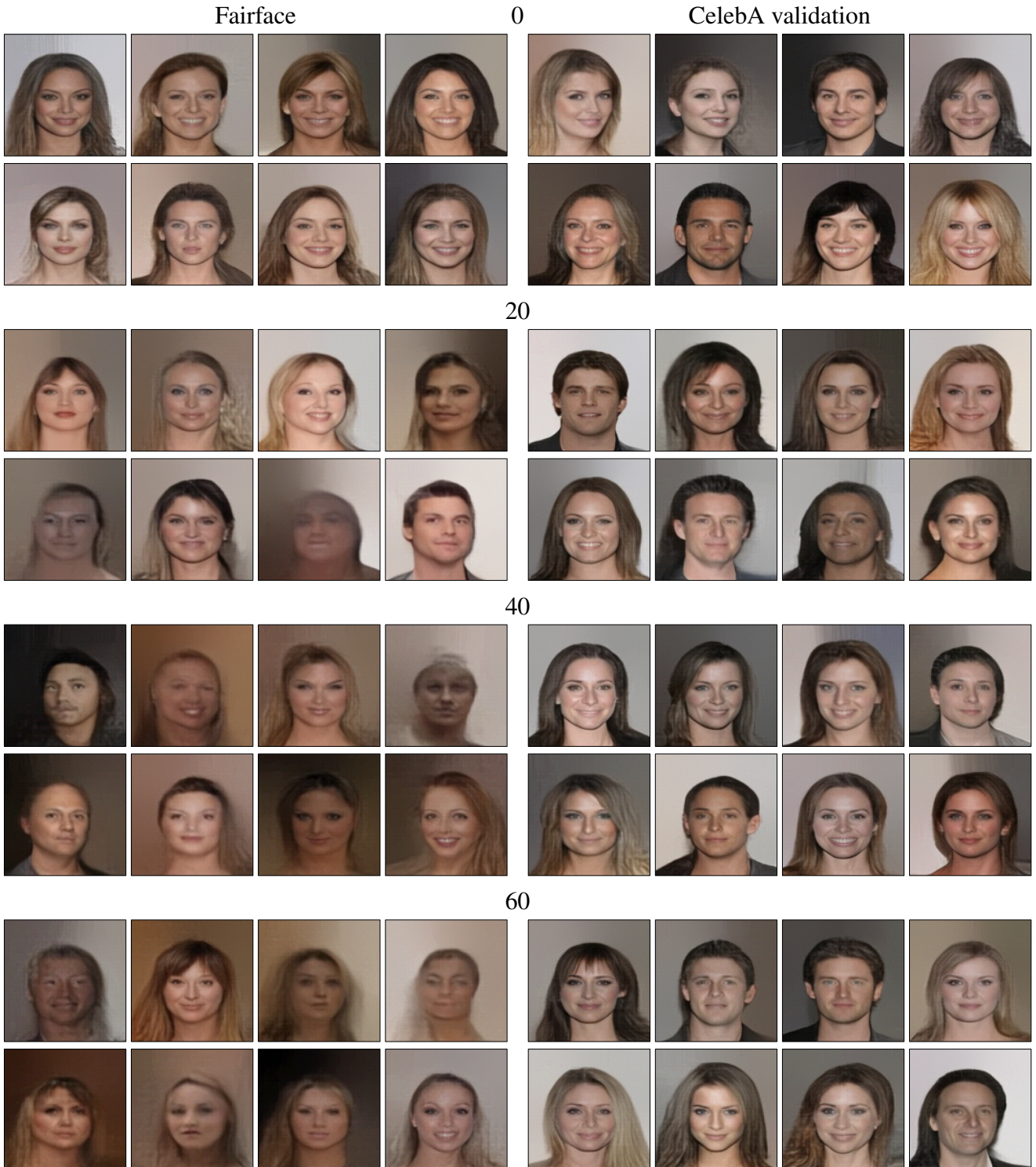


Figure C.4. **Taming with no training set.** Images generated using models that were tamed without any training data access, along the number of iterations of our method (0, 20, 40, 60). The left side shows that as the remember set is more distant than the training set (Fairface [24]), the results are worse compared to unseen data from a closer distribution (CelebA validation set).